International Journal of Geosciences, 2023, 14, 450-466
https://www.scirp.org/journal/ijg
ISSN Online: 2156-8367
ISSN Print: 2156-8359

Integrated Modelling and Reservoir Characterization of Ataga Field, Niger Delta Basin, Nigeria

Jerry Danwazan[1,2*], Kehinde Joseph Egunjobi[2,3], Richard Olorunfemi Akinwande[2]

[1]Department of Geology and Mining, Nasarawa State University, Keffi, Nigeria
[2]Department of Geology, University of Ibadan, Ibadan, Nigeria
[3]Pan African University of Life and Earth Science Institute, Ibadan, Nigeria
Email: *jerrydanwanzan@nsuk.edu.ng, *danwazanjerry1000@gmail.com, kehindee8010@gmail.com, akinwanderichardoluwafemi@gmail.com

How to cite this paper: Danwazan, J., Egunjobi, K.J. and Akinwande, R.O. (2023) Integrated Modelling and Reservoir Characterization of Ataga Field, Niger Delta Basin, Nigeria. *International Journal of Geosciences*, **14**, 450-466.
https://doi.org/10.4236/ijg.2023.145024

Received: April 17, 2023
Accepted: May 28, 2023
Published: May 31, 2023

Abstract

Integrated modelling, well correlation and petrophysical analysis were performed to characterize the reservoirs for optimum hydrocarbon correlation using 3-D seismic reflection data and suites of well logs from Ataga 5, 7, 10 and 11 wells respectively in Ataga field, shallow offshore, Niger Delta Basin, Nigeria. The study revealed the presence of two viable hydrocarbon bearing reservoirs, AT1 and AT2 and the average values of porosity, permeability, water saturation, hydrocarbon saturation, Net to Gross (NTG) and volume of shale are in the ranges of 15% - 77%, 44.5% - 75.5%, 25.5% - 85%, 15% - 75.5%, 0.70 - 0.88 and 0.11 - 0.38 respectively which goes further to show that the both reservoirs have fair characteristics that are suggestive of the presence of hydrocarbon accumulation. It can therefore be deduced that the permeability values are reflective of fair interconnectivity of pore spaces of sands within the well areas and their ability to transmit fluids, the depth and depth structural map generated for the horizons and structures shows that the most dominant trapping mechanism in the area under study is the crescentic growth fault and the rollover anticlines trending in the Northwest-Southeast direction and from the volumetric analysis. It can be deduced that the recoverable gas for AT1 and AT2 reservoirs is 2×10^6 mscf and 6×10^6 mscf respectively.

Keywords

Niger Delta, Growth Faults, Rollover Anticlines, Reservoirs, Hydrocarbon Saturation

1. Introduction

A few decades ago, oil fields were very easy to find and exploit and most of the oil fields were discovered onshore but nowadays due to the need for fossil fuel energy and depletion of onshore oil resources, offshore areas are becoming more popular. The Niger Delta is one of Africa's most producing basins, with six depobelts [1]. Thick sedimentary deposits and significant geologic features have been maintained in the basin, making it ideal for petroleum creation, migration, and entrapment from the onshore to the continental shelf and deep-water terrains. It has been verified and estimated that recoverable reserves of around 37,452 million barrels of oil [1] and 5.1 trillion cubic metres of gas resources could be found in Niger Delta hydrocarbon province [2]. After the field has been discovered through a discovery well, conventional oil field development begins and is optimized by the generation of prospect with good certainty in regards to geologic structure and rock properties such as porosity, oil saturation, permeability and other parameters obtained from the geological interpretation.

Map has been the method of representing geologic structures and rock properties but its application in reservoir geology has some inherent limitations because it is impracticable to represent 3-D reservoir heterogeneity with 2-D map [3]. Therefore, there is a need for 3-D characterization and modelling of reservoir which allows for the heterogeneous nature of the reservoir to be represented through integration of available data. Seismic and well-log data are also commonly employed to map the subsurface in petroleum exploration. Seismic profiles offer a nearly continuous lateral image of the subsurface, whereas well-logs provide precise vertical resolution of the geology at the borehole [4]. Seismic profiles can resolve structural and stratigraphic changes from reflection event arrival times and amplitudes with a high degree of precision. Reflection seismic interpretation has involved the examination of seismic properties for more than two decades. Seismic features can help with structural and stratigraphic interpretation, as well as give suggestions regarding formation type and fluid content estimation, at the same time while providing complete reservoir characterization.

This study involves integration of geophysical data interpretations to build 3-D reservoir characterization model for AT1 and AT2 reservoir in Ataga field, shallow offshore Nigeria for optimum hydrocarbon estimation. This was archived through Well log interpretation/correlation, integrated seismic interpretation of Ataga oilfield was integrated, petrophysical estimation of reservoir properties, which provided the key constrain for the definition of rock properties and also serve as input parameters for reservoir modelling. This project aimed at building AT1 and AT2-reservoir, estimating the volume of hydrocarbon accumulation in AT1 and AT2-reservoir using both map and model-based methods and comparing the hydrocarbon volumes estimated with map and model based volumetric methods.

2. Geology and Stratigraphic Setting of the Study

Ataga Field is located within the offshore Niger Delta, Nigeria (**Figure 1(a)** and **Figure 1(b)**). The Niger Delta is located in southern Nigeria, between longitudes 6˚E and 6˚E, and latitudes 4˚N and 4˚N, with an overall regressive clastic sediments thickness of about 12 km [5].

The Niger Delta is located in the Gulf of Guinea, on the West Africa Margin and spreads all through the Niger Delta province between longitude 5˚E to 8˚E and 4˚N to 6˚N [7]. The Niger Delta Basin has three formations which are the marine Akata, paralic Agbada and continental Benin Formations (**Figure 2**).

The Akata, Agbada and Benin Formations lithostratigraphic units (**Figure 2**) have been defined as the subsurface stratigraphy of the Niger Delta with its ages decreasing basinward that is, from Eocene to Pleistocene times and corresponds to Northern-Offshore depobelts which reflect an overall regressive or shoaling sequence. Generally, the formations are coarsening-upward progradational clastic deposited in marine and non-marine environments [9] [10]. The age of Akata Formation has been reported between Paleocene to Recent and its lithologies composed of shale and silts with streaks of turbidites sand [9] [10]. These shales were deposited during the early stages of Niger Delta progradation and where exposed onshore are designated as Imo Shale.

The Akata shale deposits are interpreted as deep water lowstand system tract deposits and are typically over pressured [11]. However, the Agbada Formation on the other hand has a maximum thickness of about 3500 m and occurs throughout the basin. Its lithologies consist of intercalations of sands and silts with shale stacked in prograding pattern as defined by increase in sand grains and bed thickness from bottom to the top. The age of Agbada Formation as reported is between Eocene to Pleistocene and it is interpreted to be deposited in a fluvial-deltaic environments.

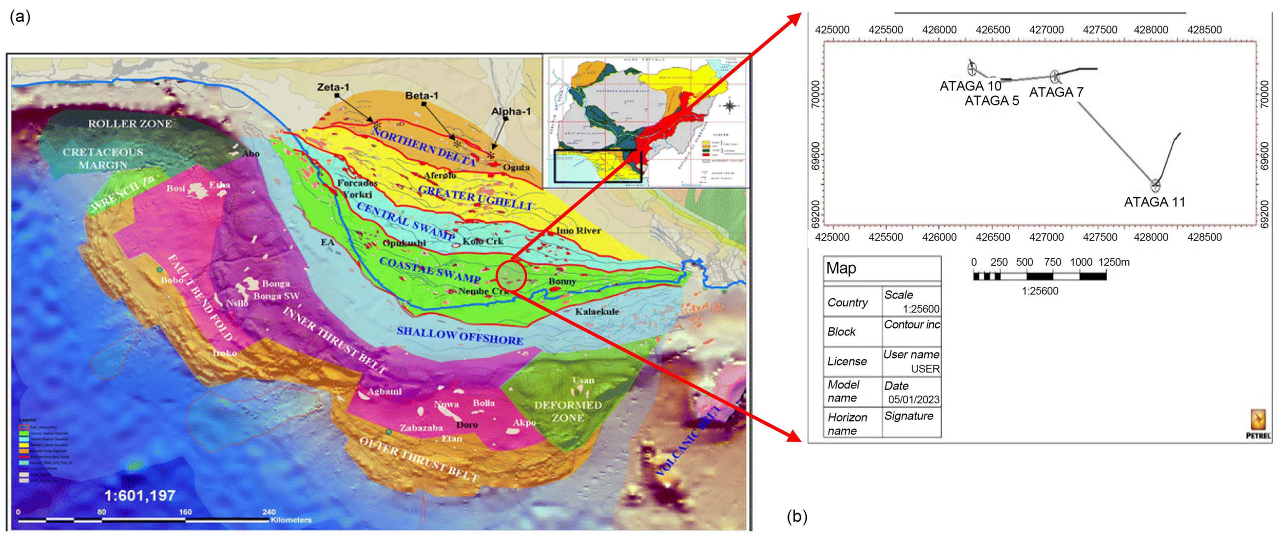

Figure 1. Location of the study area (a) Niger Delta structural framework [6] showing the study area (b) location of the wells generated from petrel map windows.

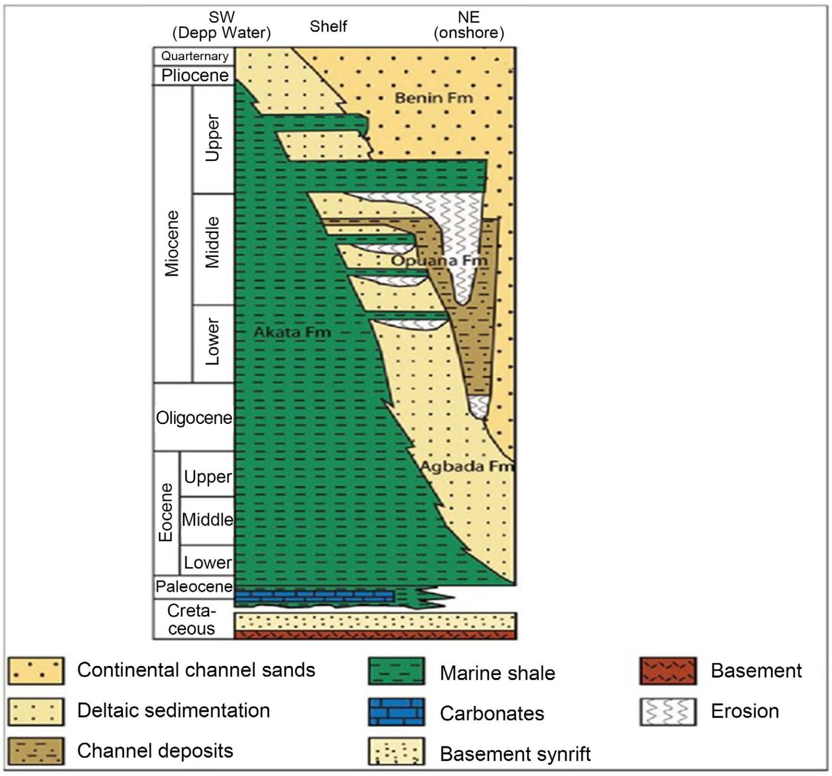

Figure 2. Regional stratigraphy of the Niger Delta [8].

The youngest formation in the Niger Delta lithostratigraphic setting is the Benin Formation, its age ranges from Oligocene to Recent and outcrop as the present delta surface. The base of Benin Formation, indicated by the youngest marine shale is placed at a depth of approximately 1500 m. The Benin Formation lithologies therefore composed of sand and have been interpreted to be deposited in an alluvial or coastal plain environment [10].

Rollover structures, multiple growth faults, antithetic faults and collapsed crest structures are the main structural features found in the Niger Delta (**Figure 3**) [7]. According to [5] and [11], structural traps were formed during synsedimentary deformation of the petroleum bearing Agbada paralic sequence. The structures become more complex towards the south with respect to gravitational instability of the under compacted, over pressured Akata Formation [7]. According to [10] hydrocarbons are trapped within the growth fault structure and about 4 billion cubic metre are present in existing field. The seal rock in the Niger Delta is primarily interbedded marine shales within the Agbada formation. Three types of seals are available: smearing of clay along faults, vertical seals and interbedded sealing layers against which subsurface reservoir sands juxtapose because of faulting [10].

3. Data and Methods

The data set given for the interpretation are well header, well logs, well deviation survey, seismic and checkshots data. The method applied for the interpretation includes using Petrel software in geological and seismic interpretation and the techlog software employed in the study of the petrophysical studies of the reservoir. The 3D seismic volume and well data were systematically loaded into the workstation for interpretation. A workflow chart summarizing the interpretation process is shown in (**Figure 4**). Well correlation was done within the "ATAGA" field with four wells as shown (**Figure 5**). The well Section window showing the correlation of the well and the reservoir across the four wells is shown with depths in SSTVD (True Vertical Depth subsea) meter from Ataga 10, Ataga 5, Ataga 7 and Ataga 11 (**Figure 5**).

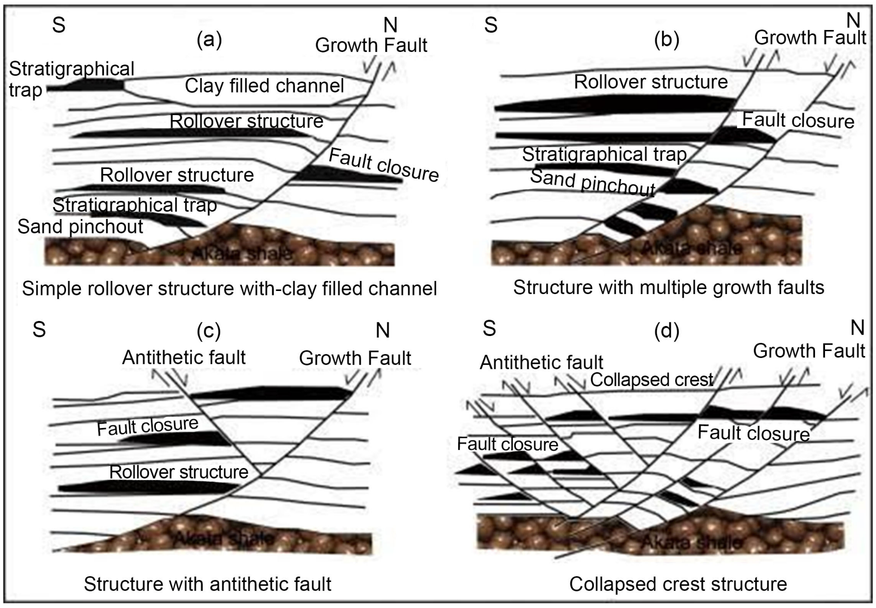

Figure 3. Examples of Niger Delta field structures and associated traps [7] and [10].

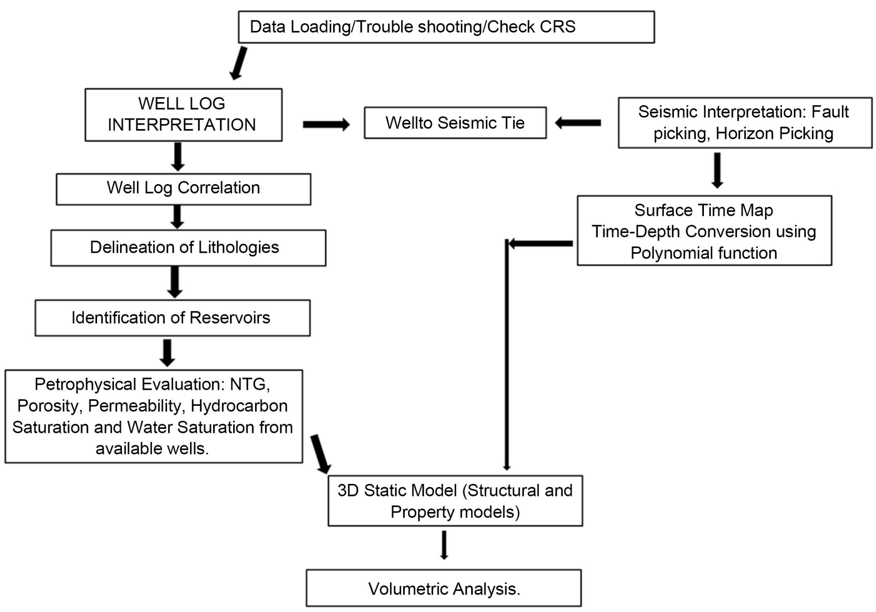

Figure 4. A workflow chart summarizing the interpretation process of Ataga field data.

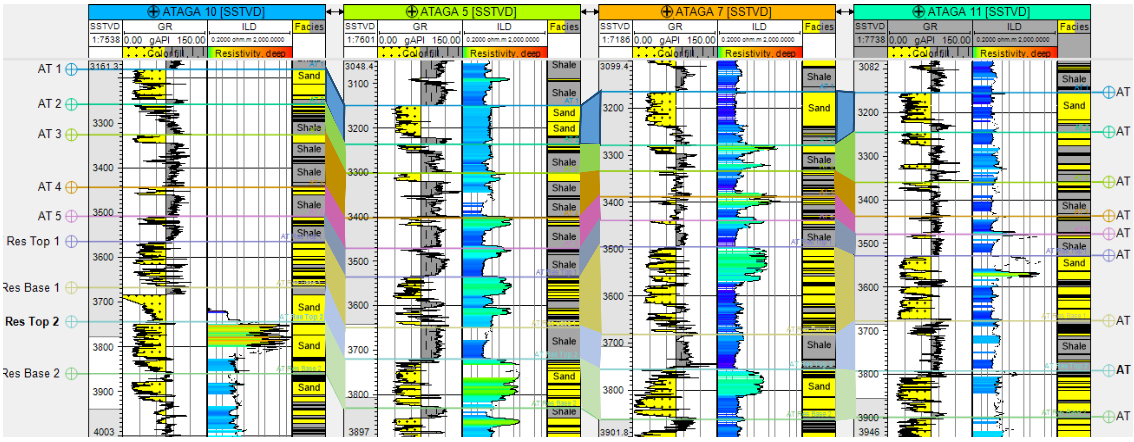

(a)

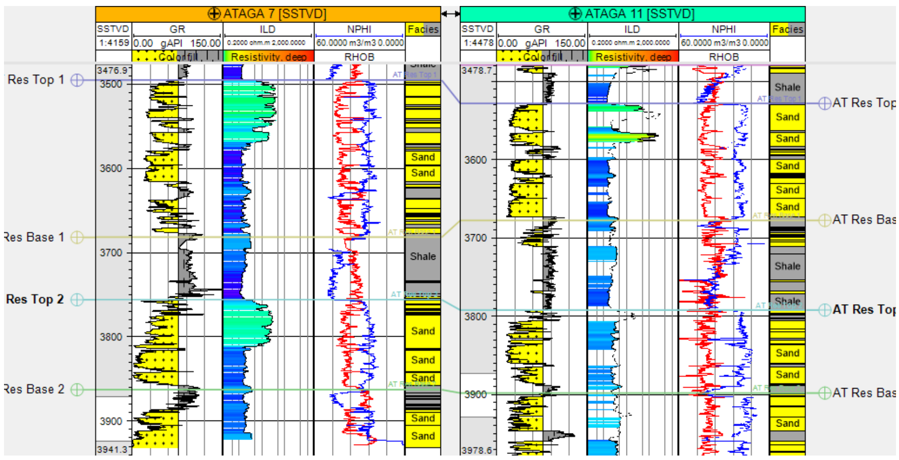

(b)

Figure 5. (a) Well correlations showing the facies log; (b) Well correlation showing reservoir AT1 and AT2 on well Ataga 10 and Ataga 5.

Horizons and faults were identified and mapped as part of the seismic data interpretation. Through seismic to well tie, the reservoir sands identified on the well-logs were traced on the seismic sections. On the seismic sections, this was done to outline the exact position, lateral extent, and shape of the reservoirs. On the inline and crossline seismic sections, the reservoir tops and bottoms on the logs were traced. On the base map, the times that corresponded to the horizons were chosen and posted. Fault interpretation, horizon interpretation, and finally seismic structural maps were constructed to analyze the geometry of the mapped horizons employed for seismic data interpretation. This was done in order to locate structural traps or closures around fault blocks.

The area extent of the reservoir is required to calculate the volume of hydrocarbon in place, but due to lack of seismic data, the values obtained will be in barrels per acre (bbl/acre [12], [13]). As a result, Equation (1) gives the volume of original oil in place (OOIP) for an oil reservoir as shown in Equations (1) and (2).

$$\text{OOIP} = \left\{7758 \times h \times \phi \times \left(1 - S_w\right)\right\} \text{l/acre} \tag{1}$$

As proposed by [13] and [14].

$$\text{STOOIP} = 7758 \times h \times \phi \times (1 - S_w) B_{oi} \text{ bbl/acre} \quad (2)$$

where B_{oi} = 1.2 bbl/STB as proposed by Osisanya *et al.*, 2021

Where h = thickness of the reservoir (in feet); ϕ = Effective porosity (in frac.); NTG = Net to Gross ratio (in frac.); S_W = Water saturation (in frac.); B_{oi} = Formation Volume Factor.

4. Results and Discussions

4.1. Results

This section captures petrophysical characteristics of two reservoirs, synthetic seismogram, structural time map and seismic section showing mapped growth faults.

Table 1. Petrophysical result for Res AT 1 and AT 2 for well Ataga 5.

Top	Bottom	avg_PHIT_D	avg_PHIE_D	avg_PERM_WR	avg_SW_AR	avg_HC	avg_VSH_GR	avg_NTG
3557.08	3649.27	0.184035	0.153553	57.46866	0.869175	0.130825	0.298937	0.701063
3741.86	3852.45	0.1699	0.157382	40.07871	0.63981	0.36019	0.125487	0.874513

Table 2. Petrophysical result for Res AT 1 and AT 2 for well Ataga 7.

Top	Bottom	avg_PHIT_D	avg_PHIE_D	avg_PERM_WR	avg_SW_AR	avg_HC	avg_VSH_GR	avg_NTG
3537.54	3680.93	0.219156	0.156836	68.91243	0.805188	0.194812	0.225336	0.774664
3798.38	3905.7	0.19727	0.152941	47.72072	0.876327	0.123673	0.155457	0.844543

Table 3. Petrophysical result for Res AT 1 and AT 2 for well Ataga 10.

Top	Bottom	avg_PHIT_D	avg_PHIE_D	avg_PERM_WR	avg_SW_AR	avg_HC	avg_VSH_GR	avg_NTG
3578.77	3666.23	0.19818	0.171704	77.91861	0	1	0.214884	0.785116
3758.24	3878.87	0.197821	0.18289	73.09433	0.522829	0.477171	0.119508	0.880492

Table 4. Petrophysical result for Res AT 1 and AT 2 for well Ataga 11.

Top	Bottom	avg_PHIT_D	avg_PHIE_D	avg_PERM_WR	avg_SW_AR	avg_HC	avg_VSH_GR	avg_NTG
3557.81	3678.04	0.236934	0.224538	167.017	0.491761	0.508239	0.113305	0.886695
3826.8	3934.2	0.245842	0.217208	151.3098	0.707331	0.292669	0.130196	0.869804

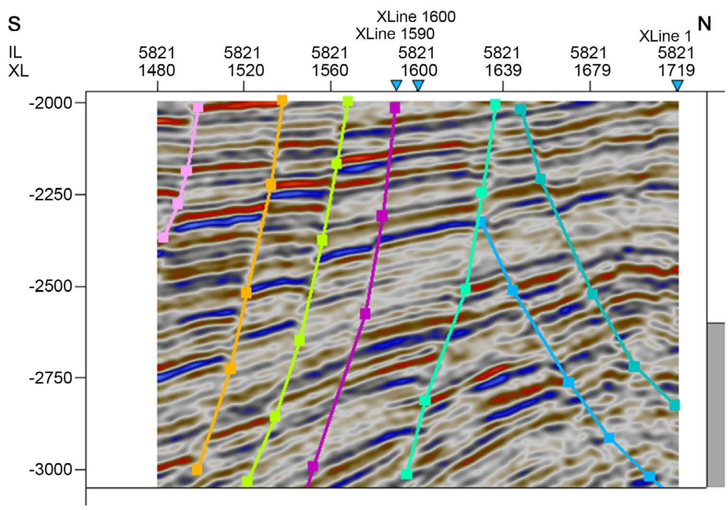

Figure 6. Inline 5821 showing faults mapped on seismic.

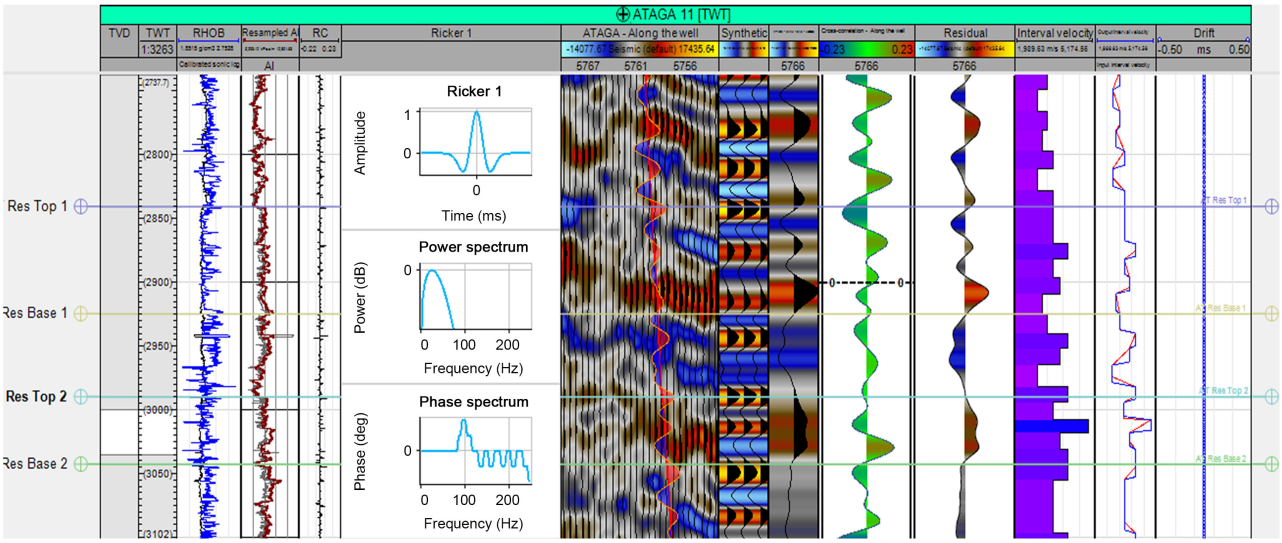

Figure 7. Synthetic seismogram showing the reservoir identified from well Ataga 11.

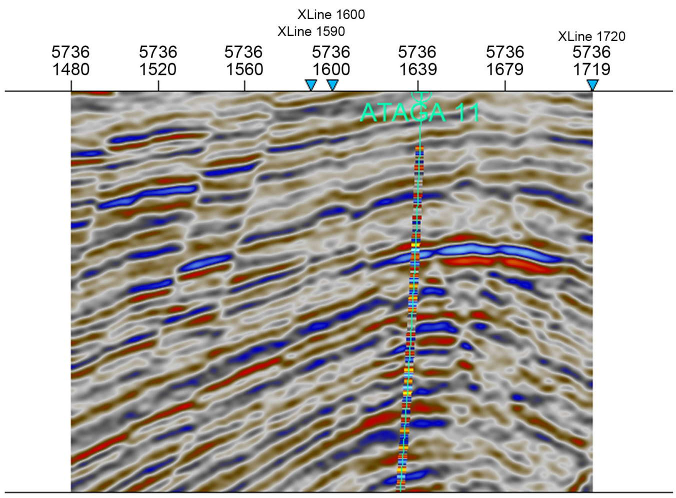

Figure 8. Well to seismic tie displayed on Seismic section.

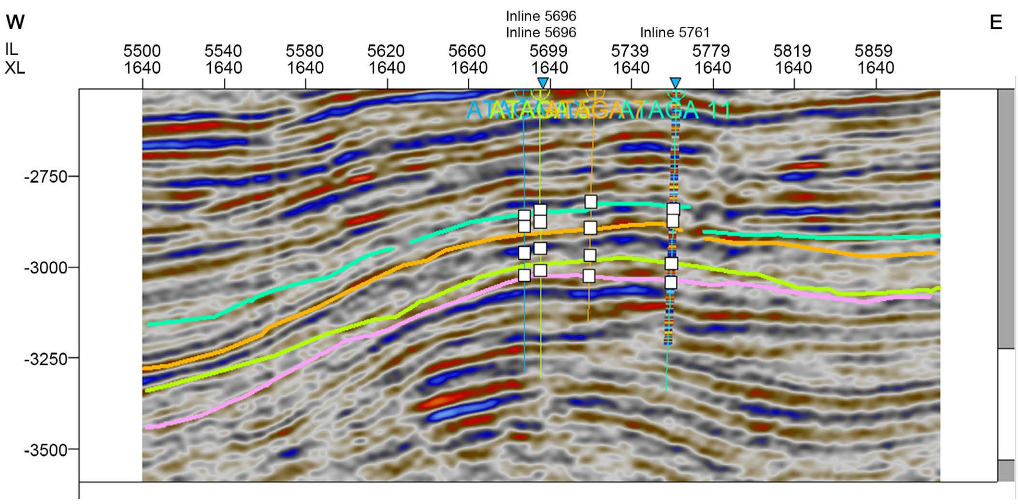

Figure 9. Horizon mapping displayed on the interpretation window.

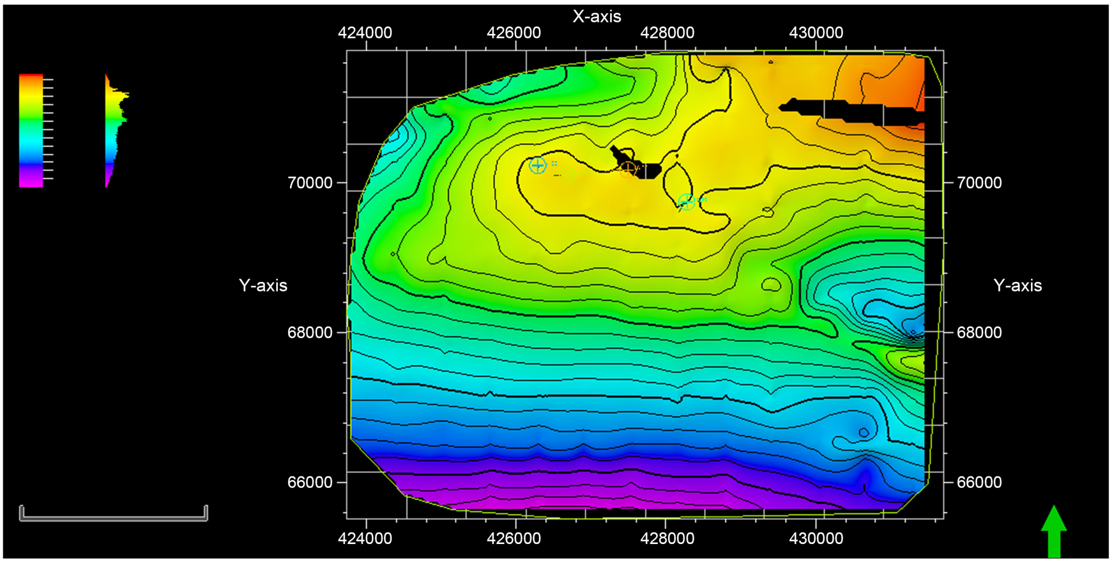

(a)

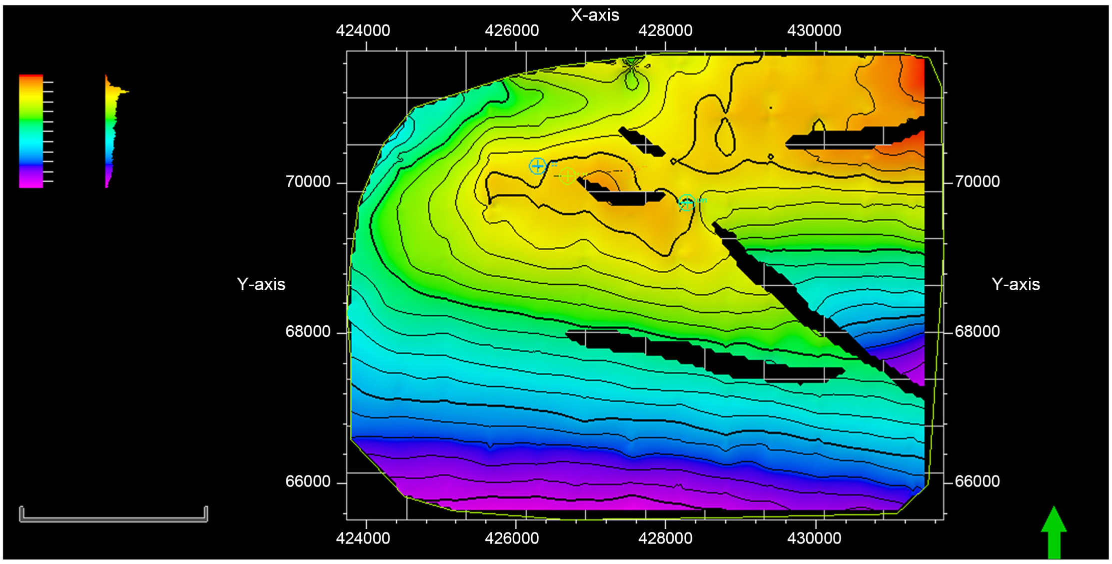

(b)

Figure 10. (a) Reservoir AT 1 Time structural map (b) Reservoir AT 2 Time structural map.

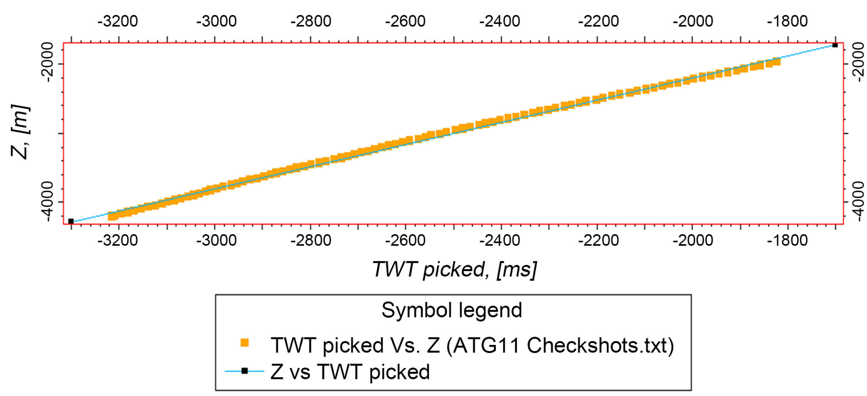

Figure 11. Polynomial function used to convert time map to depth structural map.

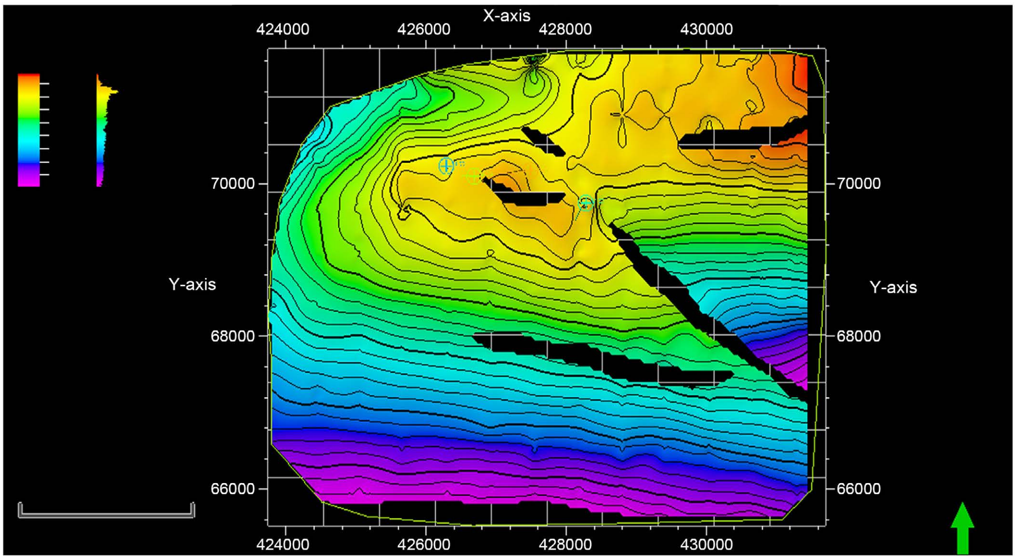

(a)

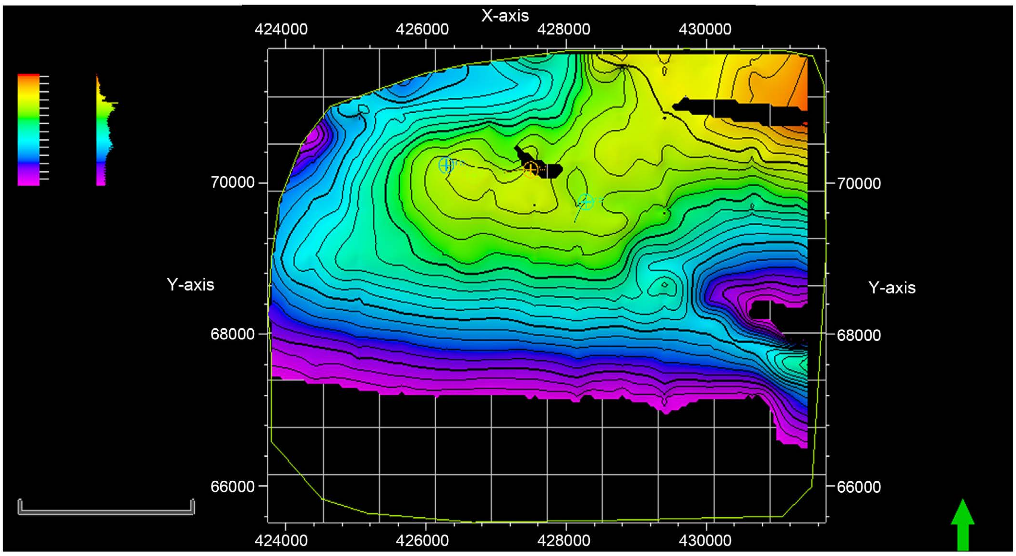

(b)

Figure 12. (a) Depth structural map of reservoir AT1 (b) Depth structural map of reservoir AT2.

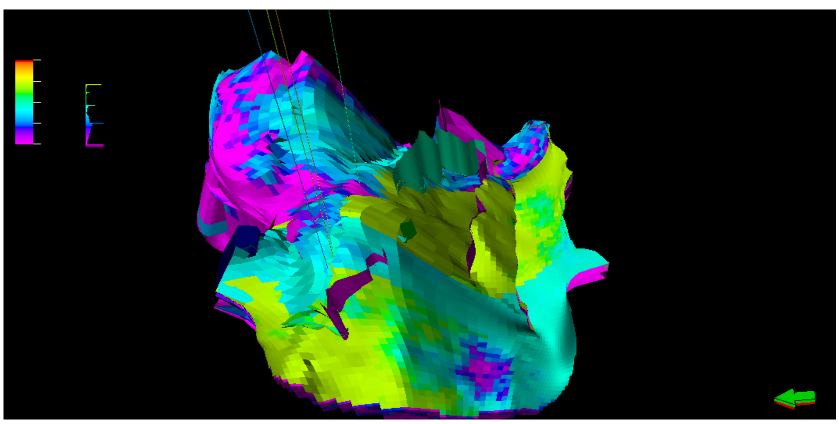

Figure 13. Permeability model of the mapped surface.

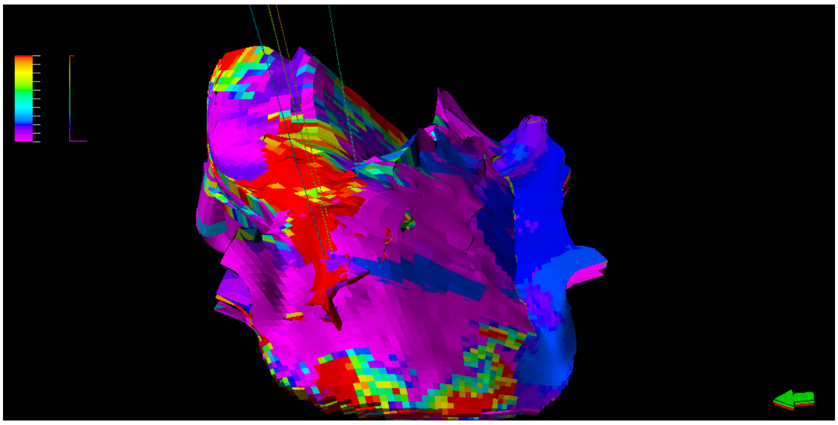

Figure 14. Effective porosity model of the mapped surface.

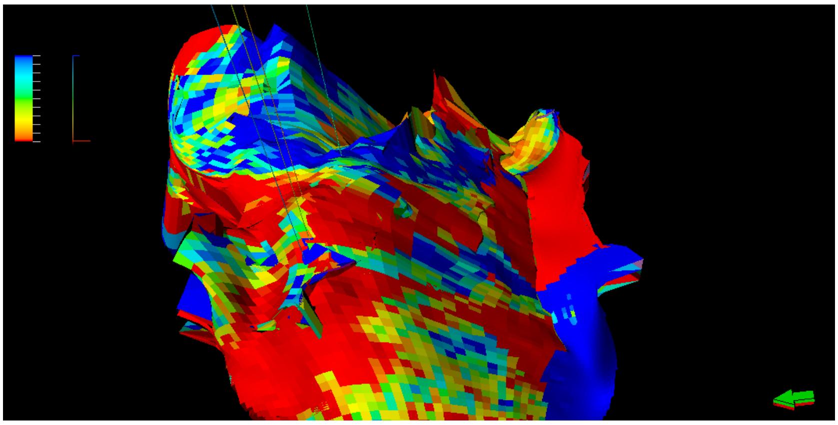

Figure 15. Water saturation model of the mapped surface.

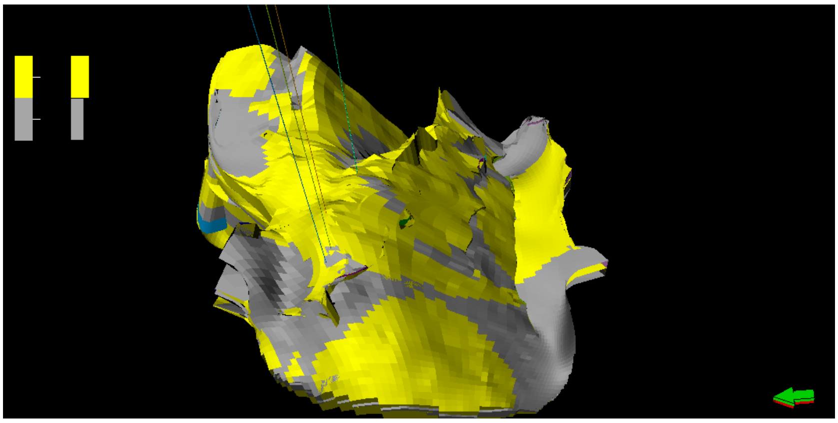

Figure 16. Facies model of the mapped surface.

Table 5. Results of volumetric analysis.

Zones	HC Area (in gas) [$\times10^6$ m^2]	Bulk volume [$\times10^6$ m^3]	Net volume [$\times10^6$ m^3]	Pore volume [$\times10^6$ MSCF]	HCPV gas [$\times10^6$ MSCF]	GIIP (in gas) [$\times10^6$ MSCF]	GIIP [$\times10^6$ MSCF]	Recoverable gas [$\times10^6$ MSCF]
AT Res Top 1	8.05	399	304	2	2	2	2	2
AT Res Top 2	12.01	1159	997	6	6	6	6	6

4.2. Discussions

4.2.1. Petrophysical Analysis

Well Ataga 5

The depth of the well log started from 1325.118 m to 4375.7088 m. Table 1 shows the summary of the petrophysical parameters of well Ataga 5, which was delineated to contain some reservoirs, but only AT 1 and AT 2 were identified as hydrocarbon-bearing with porosity ranging from 15% to 19%, water saturation 60% to 80% and hydrocarbon saturation 20% to 40%. The two reservoirs contain hydrocarbons (gas). This also depicts that porosity increases with the depth increment and water saturation decreases with an increasing depth while hydrocarbon saturation increases with an increase in depth. The reservoirs contain gas (Figure 5(b)). The average net to gross ratio (NTG) in this well is 75% with average porosity value of 17%.

The average volume of shale from this well is 0.38 while average water saturation and average hydrocarbon saturation values are 74.5% and 24.5% respectively. The average permeability value for the reservoir is 44.5%.

Well Ataga 7

The depth of the well log started from 1050.1884 m to 3975.0492 m. Table 2 shows the summary of the petrophysical parameters of well Ataga 7, which was delineated to contain some reservoirs, but only AT 1 and AT 2 were identified as hydrocarbon-bearing with porosity ranging from 15% to 17%, water saturation 80% to 90% and hydrocarbon saturation 12% to 19%. The two reservoirs contain hydrocarbons. The reservoirs contain gas. The average net to gross ratio (NTG) in this well is 80.5% with average porosity value of 15%.

The average volume of shale from this well is 0.33 while average water saturation and average hydrocarbon saturation values are 85.5% and 15.5% respectively. The average permeability value for the reservoir is 57.5%.

Well Ataga 10

The depth of the well log started from 1080.2112 m to 4335.6276 m. Table 3 shows the summary of the petrophysical parameters of well Ataga 10, which was delineated to contain some reservoirs, but only AT 1 and AT 2 were identified with hydrocarbon-bearing porosity ranging from 15% to 20%, water saturation 10% to 52% and hydrocarbon saturation 47% to 90%. The two reservoirs contain hydrocarbons. The reservoirs contain gas. The average net to gross ratio (NTG) in this well is 83% with average porosity value of 18%.

The average volume of shale from this well is 0.23 while average water saturation and average hydrocarbon saturation values are 25.5% and 75.5% respectively. The average permeability value for the reservoir is 75.5%.

Well Ataga 11

The depth of the well log started from 1192.3776 m to 4459.986 m. Table 4 shows the summary of the petrophysical parameters of well Ataga 11, which was delineated to contain some reservoirs, but only AT 1 and AT 2 were identified as hydrocarbon-bearing with porosity ranging from 21% to 24%, water saturation

45% to 70% and hydrocarbon saturation 25% to 50%. The two reservoirs contain hydrocarbons. The reservoirs contain gas. The average net to gross ratio (NTG) in this well is 86% with average porosity value of 21%.

The average volume of shale from this well is 0.11 while average water saturation and average hydrocarbon saturation values are 65.5% and 45.5% respectively. The average permeability value for the reservoir is 75.5%.

Petrophysical Properties for Reservoir AT 1

The petrophysical proportion, *i.e.* PHIE—Porosity, Sw—Water Saturation and Sh—hydrocarbon saturation of Reservoir AT 1 for well Ataga 5, Ataga 7, Ataga 10 and Ataga 11 are represented in the figure below.

The reservoir AT 1 (**Tables 1-4**) contain hydrocarbon saturation of 0.13, 0.20, 1.00 and 0.51; porosity values; of 0.15, 0.16, 0.17 and 0.22, water saturation of 0.87, 0.81, 0.00 and 0.49 in Ataga 5, Ataga 7, Ataga 10 and Ataga 11 respectively. In other words AT 1 have an average porosity of 0.18 across the four wells which are in accordance with [15] classification of porosity; porosity value of 18% is represented as fair to good reservoir. The reservoir has an average hydrocarbon saturation of 46% and average Water saturation of 54% across the four wells. It is worthy to conclude that reservoir AT 1 is fair as a reservoir for hydrocarbon and dominant fluid type is water.

Petrophysical Properties for Reservoir AT 2

The petrophysical proportion, *i.e.* PHIE—Porosity, Sw—Water Saturation and Sh—hydrocarbon saturation of Reservoir AT 2 for well Ataga 5, Ataga 7, Ataga 10 and Ataga 11 are represented in the figure below.

The reservoir AT 2 (**Tables 1-4**) contains hydrocarbon saturation of 0.36, 0.12, 0.47 and 0.29; porosity values; of 0.16, 0.15, 0.18 and 0.22, water saturation of 0.63, 0.87, 0.52 and 0.71 in Ataga 5, Ataga 7, Ataga 10 and Ataga 11 respectively. In other words AT 1 have an average porosity of 0.18 across the four wells which are in accordance with [15] classification of porosity; porosity value of 18% is represented as fair to good for a hydrocarbon reservoir. The reservoir has an average hydrocarbon saturation of 31% and average Water saturation of 68% across the four wells. It is worthy to conclude that reservoir AT 2 is poor for hydrocarbon for hydrocarbon prospect.

4.2.2. Seismic Interpretation

Structural Fault Interpretation

The structures identified during the cause of fault mapping are majorly growth fault with rollover anticlines which is typical of the structures found in the Niger Delta Basin. These growth faults mapped are found to have associated synthetic and antithetic faults which are listric in nature (**Figure 6**).

A total of nineteen (19) faults were delineated and mapped with ten (10) being major faults, five (5) being intermediate and four (4) minor faults. During the course of the mapping only eleven of these faults were found to be consistent.

These listric faults are syndepositional, exhibiting increased in stratigraphic thickening on the down thrown block or hanging wall evident by the bright and distinct signature on this side, and an increase in displacement with depth; which indicates that there were movements along the fault surface while the sediment was being deposited *i.e.* contemporaneous, The growth faults are formed by rapid sediment loading of the Agbada formation on the under compacted, over pressured, and highly mobile Akata shale.

4.2.3. Synthetic Seismogram

A synthetic seismogram is a model of a seismic trace at the borehole location It is generated by combining borehole log data (sonic and/or density) with a wavelet. The purpose of the synthetics Seismogram is to build a connection between the log data and the seismic trace which helps in correlating the well directly with a seismic section to other wells.

Well tie to Seismic was done using Ataga 11 well data and checkshot survey from Ataga 11 convolved with Ricker wavelet to generate synthetic seismograms, hence, tying the seismic to the wells. Synthetic match with seismic was quite good In Ataga 11 (**Figure 7**), mapping was done on the continuous positive polarity (Peak) beneath the zero crossing and bulk shifted, Log editor was used to despike the Ataga 11 Sonic log before performing a sonic correction because poor quality log input to the synthetic seismogram generation can give Inconsistent results. For instance spiky sonic logs (cycle skipping) results in artificial events in the synthetic trace that can be mistaken for real reflectors. This reason leads to despiking the sonic log in order to remove the spike values.

Horizon Mapping

The mapping of the horizon was based on synthetic seismogram generated (**Figure 8**). The key seismic reflections which corresponded to top of main reservoir sands were identified on seismic data for mapping. Four horizons corresponding to the top and base of the reservoir were mapped as AT 1 and AT 2 (reservoir tops and base) (**Figure 9**). Horizons were picked on inlines and crosslines.

From the time map (**Figure 10(a)**, **Figure 10(b)**), depth map was generated using polynomial function (**Figure 11**) and depth-structural maps generated for the horizons and structures picked across the study area (**Figure 12(a)**, **Figure 12(b)**) it shows that most dominant trap was the crescentic growth fault generated rollover anticlines trending Northwest, Northeast-Southwest. [16] discussed that the presence of roll-over Structures may indicate possible hydrocarbon accumulation in the vicinity of such roll over structures.

3-D Static Geological Model

Geological modelling or static modelling involves populating the reservoir architecture (Structure and Stratigraphy) with rock properties. [17] in view of the necessity of dynamic simulation process and to arrive at a final well and production behavior, it was necessary to build a static model that represented as closely as possible the subsurface reality of the Sand 1, and 2 that have been encountered by most wells [18].

The 3D seismic structural interpretation, property models like the porosity, permeability, water saturation and net to gross models from log analyses were used to build the static model. The PETREL (Version 2018) suite was used in building the static model.

Structural Model

This (in Petrel) involves Fault Modelling, Pillar Gridding and Horizon Making. Fault Modelling involved definition of the various faults in the model which formed the basis for generating the 3D Grid. This field is bounded by synthetic and antithetic growth faults. The faults used in this study were named major, intermediate and minor faults respectively. The faults were built using key pillars and joints of these key pillars formed the fault plane. These faults defined breaks in the 3D grid. The structural model was based on the depth-converted 3D seismic interpretation.

Permeability Model: The map underscores fair permeability values which range from 50 mD to 170 mD within the well area of Ataga field using Sequential Gaussian Simulation algorithm as shown in the (**Figure 13**) below. The values are reflective of fair interconnectivity of pore spaces of the sand within the well area and their ability to transmit fluids.

Porosity Model: The map shows the prominence of good porosity distribution (0.16 - 0.21) within well area of the Ataga field using Sequential Gaussian Simulation algorithm as shown in the (**Figure 14**). This indicates the pore spaces have less space to accommodate fluid.

Water Saturation Model: The map reveals that water saturation distribution within the well area of the Ataga field using Sequential Gaussian Simulation algorithm below varies from 0.49 to 0.87. This is indicative of more of water than hydrocarbon (**Figure 15**).

Facies Model: The map shows that the distribution of facies within the Ataga field using Truncated Gaussian Simulation algorithm is showed that variation of sand to shale ranges from 40% - 60%. (**Figure 16**) This shows that the reservoir sands present in the field are minimal.

Volumetric Analysis

For the volumetric analysis, the fluid contacts generated from the mapped horizons were used (**Table 5**). From the volumetric analysis, it can be deduced that the recoverable gas for AT1 and AT2 reservoirs is 2×10^6 mscf and 6×10^6 mscf respectively (**Table 5**).

5. Conclusion

The study revealed the presence of two viable hydrocarbon bearing reservoirs, AT1 and AT2. The result has shown that the average values of porosity, permeability, water saturation, hydrocarbon saturation, Net to Gross (NTG) and volume of shale are in the ranges of 15% - 77%, 44.5% - 75.5%, 25.5% - 85%, 15% - 75.5%, 0.70 - 0.88 and 0.11 - 0.38 respectively. The findings gotten from petrophysical measurements carried out on the AT1 and AT2 have revealed that both reservoirs have fair characteristics that are suggestive of the presence of hydrocarbon accumulation. From the volumetric analysis, it can be deduced that the recoverable gas for AT1 and AT2 reservoirs is 2×10^6 mscf and 6×10^6 mscf respectively. The permeability values are reflective of fair interconnectivity of pore spaces of sands within the well areas and their ability to transmit fluids. The depth and depth structural map generated for the horizons and structures shows that the most dominant trap mechanism is the crescentic growth fault and the rollover anticlines trending in the Northwest-Southeast direction. It can therefore be said that both in structural and stratigraphic mapping, the combination of seismic data and well logs has proven to be reliable and valid tool.

Acknowledgements

We wish to acknowledge Schlumberger for making available the software that helped in the modelling of the reservoirs and other simulation works carried out in this research. We also wish to appreciate the Departments of Geology Nasarawa State University, Keffi and that of University of Ibadan, Nigeria for creating the enabling environment for the successful research.

Conflicts of Interest

The authors declare no conflicts of interest regarding the publication of this paper.

References

[1] Organization of the Petroleum Exporting Countries (2017) Annual Statistical Bulletin. http://www.opec.org/opec_web/en/publications/202.htm

[2] Fajana, A.O., Ayuk, M.A., Enikanselu, P.A. and Oyebamiji, A.R. (2018) Seismic Interpretation and Petrophysical Analysis for Hydrocarbon Resource Evaluation of 'Pennay' Field, Niger Delta. *Journal of Petroleum Exploration and Production Technology*, **9**, 1025-1040. https://doi.org/10.1007/s13202-018-0579-4

[3] Deutsch, C.V. and Journel, A.G. (1998) Geostatistical Modeling. Oxford University Press, New York.

[4] Singh, R.J., Kharo, H.L., Saha, P., Singh, S.N. and Chandra, M. (1997) Integration of Well and 3D Seismic Data for Prospect Evaluation: A Case Study. *Geohorizons*, **11**, 1-9.

[5] Evamy, B.D., Haremboure, J., Kamerling, P., Knaap, W.A., Molloy, F.A. and Rowlands, P.H. (1978) Hydrocarbon Habitat of Tertiary Niger Delta. *American Association of Petroleum Geologists Bulletin*, **62**, 1-39. https://doi.org/10.1306/C1EA47ED-16C9-11D7-8645000102C1865D

[6] Ejedavwe, J., Fatumbi, A., Ladibo, K. and Stone, K. (2002) Pan-Nigeria Exploration Well Look Back (Post-Drill Well Analysis). Shell Petroleum Development Company of Nigeria. Exploration Report 2002.

[7] Tuttle, W.L., Charpentier, R.R. and Brownfield, M.E. (1999) The Niger Delta Petroleum System: Niger Delta Province, Nigeria, Cameroon and Equatorial Guinea, Africa. Open-File Report 99-50-H. United States Geological Survey. Denver Colorado. https://doi.org/10.3133/ofr9950H

[8] Lawrence, S.R., Munday, S. and Bray, R. (2002) Regional Geology and Geophysics of the Eastern Gulf of Guinea (Niger Delta to Rio Muni). *The Leading Edge*, **21**, 1112-1117. https://doi.org/10.1190/1.1523752

[9] Weber, K.J. and Daukoru, E.M. (1975) Petroleum Geology of the Niger Delta. *Journal of Mining and Geology*, **12**, 9-12.

[10] Doust, H. and Omatsola, E. (1990) Niger Delta. In: Edwards, J.D. and Santogrossi, P.A., Eds., *Divergent/Passive Margin Basins*, American Association of Petroleum Geologists, Tulsa, 239-248. https://doi.org/10.1306/M48508C4

[11] Stacher, P. (1995) Present Understanding of the Niger Delta Hydrocarbon Habitat. In: Oti, M.N. and Postma, G., Eds., *Geology of Deltas*, A.A. Balkema, Rotterdam, 257-267.

[12] Osisanya, W.O., Alile, O.M., Eze, S.U., Ibitoye, T.A. and Oyanameh, O.E. (2021) Hydrocarbon Play Assessment of "Oswil" Field, Onshore Niger Delta Region. *Journal of Geological Research*, **3**, 11-21 https://doi.org/10.30564/jgr.v3i1.2783

[13] Ochoma, U., Uko, E.D. and Horsfall, O.I. (2020) Deterministic Hydrocarbon Volume Estimation in the Onshore Fuba Field Niger Delta, Nigeria. *Journal of Applied Geology and Geophysics*, **8**, 34-40.

[14] Udegbunam, E.O. and Ndukwe, K. (1988) Rock Property Correlation for Hydrocarbon Producing Sand of the Niger Delta Sand. *Oil & Gas Journal*, **2**, 11-22.

[15] Baker, H.I. (1992) Advanced Wireline and MWD Procedures Manual. B.H.I Technical Publications Group.

[16] Weber, K.J. and Daukoru, E. (1975) Petroleum Geology of the Niger Delta. *Journal of Mining and Geology*, **12**, 9-12.

[17] Oladipo, M.K. (2011) Integrated Reservoir Characterization: A Case Study of an Onshore Reservoir in Niger Delta Basin. Ph.D. Thesis, Faculty of the African University of Science and Technology, Abuja.

[18] Adeoti, L., Adesanya, O.Y, Oyedele, K.F., Afinotan, P. and Adekanle, A. (2017) Lithology and Fluid Prediction from Simultaneous Seismic Inversion over Sandish Field, Niger Delta, Nigeria. *Geosciences Journal*, **22**, 155-169. https://doi.org/10.1007/s12303-017-0018-4